Appendix G

Probabilistic Plume Modeling

Appendix G

Probabilistic Plume Modeling

G-1. Overview

The trends observed in the statistical evaluations of the field data, while intuitive, are empirical owing to the nature of the analyses. Reconciliation of these empirical findings with conceptual mathematical models of plume behavior can provide a theoretical basis for interpreting the observations. Given the emphasis of the present study on identifying and quantifying relationships between averaged site hydrogeologic variables and plume variables defined in a broad context, analytical solutions are highly suitable models for a probabilistic approach. They also produce simplified representations of plume behavior that are readily amenable to statistical analyses. In this context, the heterogeneity in the groundwater flow field, which often severely limits the application of analytical solutions, may be addressed through the macrodispersion coefficients.

Domenico (1987) presented a solution for concentration, C, as a function of x, y, and t, which also accounts for the effects of dispersion in the vertical direction:

$$C(x,y,t) = \left(\frac{C_0}{8}\right)\exp\left\{\left(\frac{x}{2\alpha_x}\right)\left[1-\left(1+\frac{4R\lambda\alpha_x}{v}\right)^{1/2}\right]\right\} \bullet \operatorname{erfc}\left[\frac{x-\frac{v}{R}t\left(1+4R\lambda\alpha_x/v\right)^{1/2}}{2\left(\alpha_x\frac{v}{R}t\right)^{1/2}}\right] \quad \text{(Eq. G-1)}$$

$$\bullet\left\{\operatorname{erf}\left[\frac{(y+Y/2)}{2(\alpha_y x)^{1/2}}\right]-\operatorname{erf}\left[\frac{(y-Y/2)}{2(\alpha_y x)^{1/2}}\right]\right\} \bullet \left\{\operatorname{erf}\left[\frac{Z}{2(\alpha_z x)^{1/2}}\right]-\operatorname{erf}\left[\frac{-Z}{2(\alpha_z x)^{1/2}}\right]\right\}$$

Here, C_0 refers to a vertical rectangular-source (dimension Y x Z), of solute concentration along the upstream boundary, v the uniform groundwater velocity in the x-direction, α_x, α_y, and α_z the respective longitudinal, transverse, and vertical transverse dispersivities, R the retardation coefficient, and λ the first-order transformation rate. This solution is only valid for a semi-infinite homogeneous aquifer. From. Eq. G-1, the plume's length along the x-axis may be estimated by setting $y = 0$ and C equal to some specific contour interval (i.e., $C = 10$ ppb), and solving for x using a suitable numerical approach (in this case a bisection search algorithm).

Application of Monte Carlo simulation techniques to analytical solute transport models can provide valuable insights into factors affecting plume behavior when combined with population studies of existing groundwater plumes. Monte Carlo analyses are routinely used in engineering probability forecasting applications (e.g., Ang and Tang, 1984). Woodbury et al. (1995) discussed the use of Monte Carlo analyses in practical ground water engineering applications. The main reason for resorting to a probabilistic analysis of phenomena of transport making use of a mathematical model stems from the lack of sufficient field data on site-specific features of plume

behavior.   Probabilistic modeling of contaminant transport involves utilizing user-specified probability distributions of physical and chemical model variables, based on available data, to produce forecasts through multiple Monte Carlo realizations. The Monte Carlo approach allows uncertainties in hydrogeological data (e.g., hydraulic conductivity, hydraulic gradient (magnitude and direction), nature of the source, and chemical data (e.g., degradation rates) to be translated into uncertainties regarding plume extents and rates of growth.   Sensitivity analyses based on comparing uncertainties in input variables to the variance in corresponding forecast results may provide insight into the critical data for quantifying the behavior of plumes.

G-2. Parameter Distributions

For the modeling analysis, synthetic plumes were generated using random combinations of the variables in Eq. G-1. The values of these variables were constrained by probability distributions developed from field data (Table G-1). Probability distributions of groundwater velocity were obtained by Darcy's law for ranges of K and ∇h values noted at sites included in the study. Similarly, a probability distribution for C_0 could be estimated from the ranges of maximum historical concentrations.   In this case, values of C_{max}, representing maximum measured concentrations, were chosen from the overall C_{max} probability distribution observed in the field data set. For each synthetic plume realization, this value was assumed to represent 10% of the actual boundary concentration, C_0, based on the 10% saturation rule-of-thumb for inferring the presence of DNAPL (Feenstra and Cherry, 1988). Thus the geometric mean value of the C_0 probability distribution is a factor of ten higher than the C_{max} distribution, although the standard deviation is identical.

Ranges of other variables (e.g., R, α_x, α_y, t), while not well-constrained by the database, can be assumed within reason using best professional judgment. The retardation coefficient, R, for example, may be calculated from the relationship,

$$R = 1 + \frac{K_{oc} f_{oc} \rho_b}{\phi}$$ (Eq. G-2)

where K_{oc} is the organic carbon partitioning coefficient, f_{oc} is the fractional organic carbon content, ρ_b the bulk density, and ϕ the porosity. The probability distribution of f_{oc} could not be determined from the site database because of a paucity of data. Instead, a probability distribution was postulated (Fig. G-1) from a published distribution of f_{oc} values observed at a number of field sites (Wiedemeier et al., 1997).   First-order degradation rates ranging from $\lambda = 0.7$ to $\lambda = 0.07$ year^{-1}, corresponding to half-lives from 1 year to 10 years, were chosen from an informal survey of reported values in the literature (the survey of reductive dehalogenation rates of TCE by Aronson and Howard (1997) recommends half-lives of 1.2 years to 13.2 years as conservative estimates). Half of the synthetic plumes were assigned degradation rates within this range, while the remainder of the plumes were assigned a degradation rate of $\lambda = 0$ as a control set representing stable CVOCs.

G-3. Model Results

The output of the Monte Carlo simulations consisted of a distribution of plume lengths, each corresponding to a unique set of random input variables chosen from the defined probability distributions. A total of 2000 realizations were developed. To mimic the results of the field data analyses as much as possible, only simulated plumes with lengths falling within the range of observed plume lengths (approximately 100 feet to 10,000 feet) were included in the analysis. To simulate the size of the field data set, 100 plumes were drawn at random from the transforming population and the stable population each. Relationships between plume length and C_{max} (assumed equal to 1/10 the C_0 value for each realization) as well as plume length and specified site groundwater velocity, v, are shown for all synthetic plumes on Figures G-2 and G-3, respectively. The scatter evident in both relationships illustrates the effect of multiple variables on plume length, even under ideal conditions (uniform groundwater velocity field, Fickian-type dispersion, uniform transformation rate, isotropic two-dimensional aquifer, and constant boundary conditions). The relationship between plume length and C_{max} reproduces the scatter observed in the field data fairly well (Appendix A, Fig. A-1). In contrast, much more scatter is evident in the field data with respect to the plume-length-versus-velocity relationship (Appendix A, Fig. A-3) than in the simulated plume set. The explanation for this difference is likely to stem from the difficulty in defining a mean site groundwater velocity for a real field site, in contrast to the specified (known) uniform velocities characterizing the synthetic plumes.

Synthetic plume length distributions for transforming and stable CVOC plumes are shown on Fig. G-4 (top). These results are very similar to analysis of the field data; transformations appear to exert little influence on raw plume lengths above the noise in the data caused by other factors. However, the definition of a plume length index for the synthetic plumes in a manner analogous to the measured plume lengths (Appendix A, Eq. A-1) produces a significant separation of the two probability distributions (Fig. G-4, bottom). This analysis procedure and the results are consistent with those associated with the field data. The findings thus support the conclusion that source strength and groundwater velocity exert a strong enough influence on plume length to be directly discernible. In contrast, transformation rates are slow enough so that plume length effects cannot be easily identified above the noise associated with plume data without normalization procedures.

Rank-based correlation coefficients quantifying the relationships between plume length, the plume length index as defined in Appendix A, and the various model variables are shown in Table G-2. The correlation coefficients indicate the importance of groundwater velocity variability and variability in the boundary concentration in influencing plume length relative to other variables. Dividing plume length by v and C_{max} reduces the effects of these two variables, so that the correlations between other variables such as λ and the plume length index improve. This may explain why the plume length index concept is successful at identifying differences between the plumes from the No RD and Strong RD groups; the indexing procedure improves the correlation of plume extent with the rate of transformation.

Best-fit lognormal frequency distributions of input parameters (maximum concentration and groundwater velocity) and output metrics (plume length and plume length indices) are shown on Figure G-5 for the synthetic plume population, with the same distributions gleaned from the field data shown as a summary comparison. The capacity of the model to capture the average behavior of plumes in the data set is encouraging, providing support to the notion that site-specific effects tend to average out over a large number of sites, so that general trends do become apparent.

Ultimately, the modeling results, the field data, and the general linear model development (Appendix C) all convey the possibility of examining plume populations as multivariate systems (Figs. G-6 and G-7). Models of such systems would link measurable aspects of plume behavior, such as length, to linear combinations of variables (or log variables) in a statistical sense. Powerful new insights could be gleaned into plume behavior, provided that a large enough data set could be assembled to allow analyses of distinct regions of variable space. In the examples given in Figs. G-6 and G-7, the multivariate relationship between plume length, groundwater velocity, and maximum concentration suggests a much stronger role for velocity in influencing plume length in the synthetic plume population than in the field data. This may stem from a deficiency in our capacity to accurately quantify a true mean groundwater velocity for field sites, as the modeled plumes are all based on an assumption of a uniform flow field which is known precisely. As such, this may suggest the need to use geostatistical approaches in future analyses which quantify the uncertainties associated with groundwater velocity at field sites in the data set.

References

Ang, A. H. S, and W. H. Tang (1984), *Probability Concepts in Engineering and Planning Design, Vol. 2 : Decision, Risk, and Reliability* (Wiley, New York).

Aronson, D., and P. H. Howard (1997), "Anaerobic Biodegradation of Organic Chemicals" in *Groundwater: A Summary of Field and Laboratory Studies, Draft Final Report, prepared for the American Petroleum Institute*, Washington, D. C.

Domenico, P. A. (1987), "An analytical model for multidimensional transport of a decaying contaminant species," *Journal of Hydrology* **91**, 49–58.

Feenstra, S., and J. A. Cherry (1988), "Subsurface contamination by dense non-aqueous phase liquid (DNAPL) chemicals," in *Proceedings of the International Groundwater Symposium, International Association of Hydrogeologists*, May 1–4, Halifax, Nova Scotia, 62–69.

Wiedemeier, T. H., M. A. Swanson, D. E. Moutoux, E. K. Gordon, J. T. Wilson, B. H. Wilson, D. H. Kampbell, J. E. Hansen, P. Haas, and F. H. Chapelle (1997), "Technical Protocol for Evaluating Natural Attenuation of Chlorinated Solvents," in *Groundwater, prepared for the Air Force Center for Environmental Excellence, Technology Transfer Division*, Brooks Air Force Base, San Antonio, Texas.

Woodbury, A., F. Render, and T. Ulrych (1995), "Practical probabilistic groundwater modeling," *Ground Water*, **33**(4), 532–538.

Table G-1. Transport model parameter probability distributions.

Parameter	Distribution	Basis
Maximum concentration (ppb), C_0	Lognormal. 10th-percentile: 29 90th-percentile: 23,750	Lognormal distribution fit to observations, uniformly multiplied by 10.
Source area width (ft), Y	Uniform. 5-60	Postulated.
Source area depth (ft), Z	Uniform. 5-60	Postulated.
Hydraulic conductivity (ft/day), K	Lognormal. 10th-percentile: 0.19 90th-percentile: 246	Lognormal observations fit to geometric mean values from each site[1].
Hydraulic gradient, ∇h	Lognormal. 10th-percentile: 0.0011 90th-percentile: 0.0614	Lognormal observations fit to reported values from each site
Porosity, ϕ	Normal. 0.25 ± 0.03	Postulated.
Fractional soil organic carbon, f_{oc}	Lognormal. 10th-percentile: 0.01% 90th-percentile: 1%	Postulated.
Transformation half-life (yrs), $t_{1/2}$	Uniform. 1-10	Postulated; based on an informal review of literature values.
Ratio of longitudinal dispersivity, α_x, to plume length	Lognormal. 10th-percentile: 0.033 90th-percentile: 0.33	Postulated; based on the common assumption of the ratio of α_x to plume length ~ 10%.
Ratio of longitudinal dispersivity, α_y, to plume length	Lognormal. 10th-percentile: 0.0033 90th-percentile: 0.033	Postulated; based on the common assumption of the ratio of α_y to α_x ~ 10%.
Ratio of longitudinal dispersivity, α_z, to plume length	Lognormal. 10th-percentile: 1.67×10^{-3} 90th-percentile: 1.67×10^{-2}	Postulated.
Elapsed time since release (yrs), t	Uniform. 10-50	Postulated; informally based on typical reported site use histories.

---

[1]Based on reported pumping test or slug test results.

Table G-2. Rank correlation coefficients (Spearman's *r*) between simulated plume length and plume length indices and model variables.

Variable	Rank correlation coefficent with respect to L	Rank correlation coefficent with respect to PLI
Groundwater velocity, *v*	0.73	–
Maximum concentration, C_{max}	0.32	–
Retardation coefficient, *R*	-0.20	-0.32
Ratio of vertical dispersivity to plume length, $\alpha_z{:}L$	-0.20	0.06
First-order degradation coefficient, λ	-0.12	-0.21
Ratio of longitudinal dispersivity to plume length, $\alpha_x{:}L$	0.06	0.15
Transverse extent of source area, *Y*	-0.04	0.25
Vertical extent of source area, *Z*	-0.04	0.18
Ratio of transverse dispersivity to plume length, $\alpha_y{:}L$	-0.01	-0.16
Elapsed time since source term initiation, *t*	0.00	-0.01
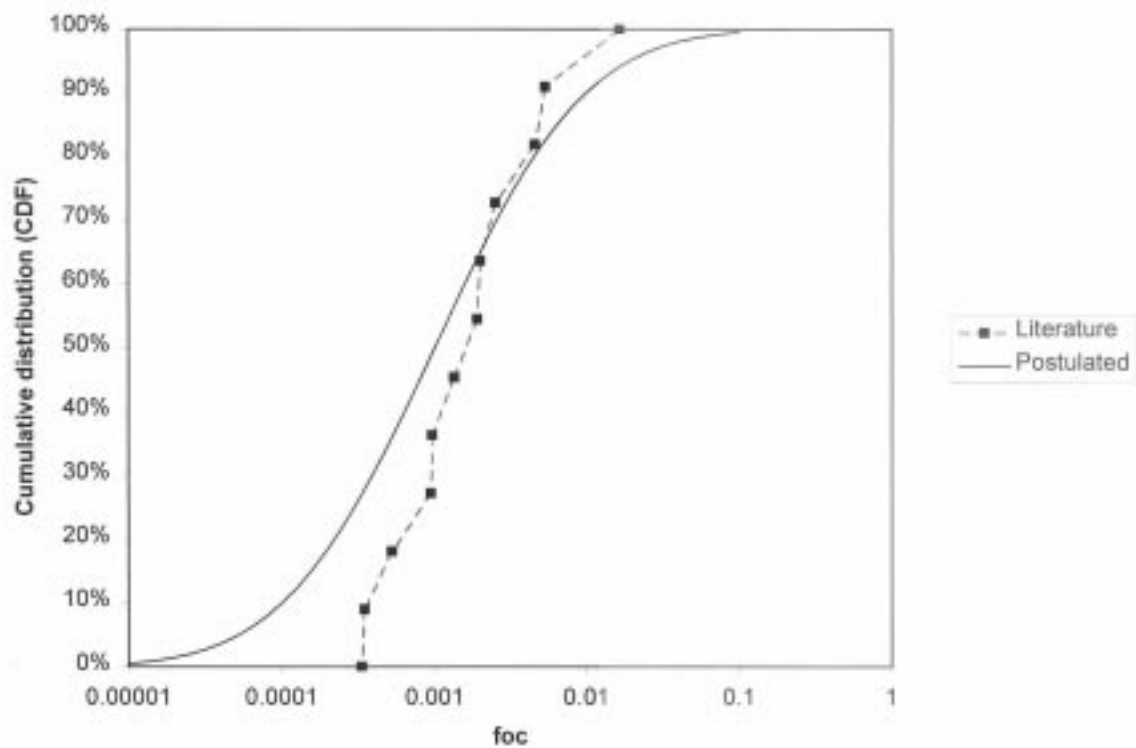
Figure G-1. Cumulative distributions of organic carbon content developed from analysis of reported field measurements (Weidemeier et al., 1997) and the lognormal distribution used in the Monte Carlo plume simulations.
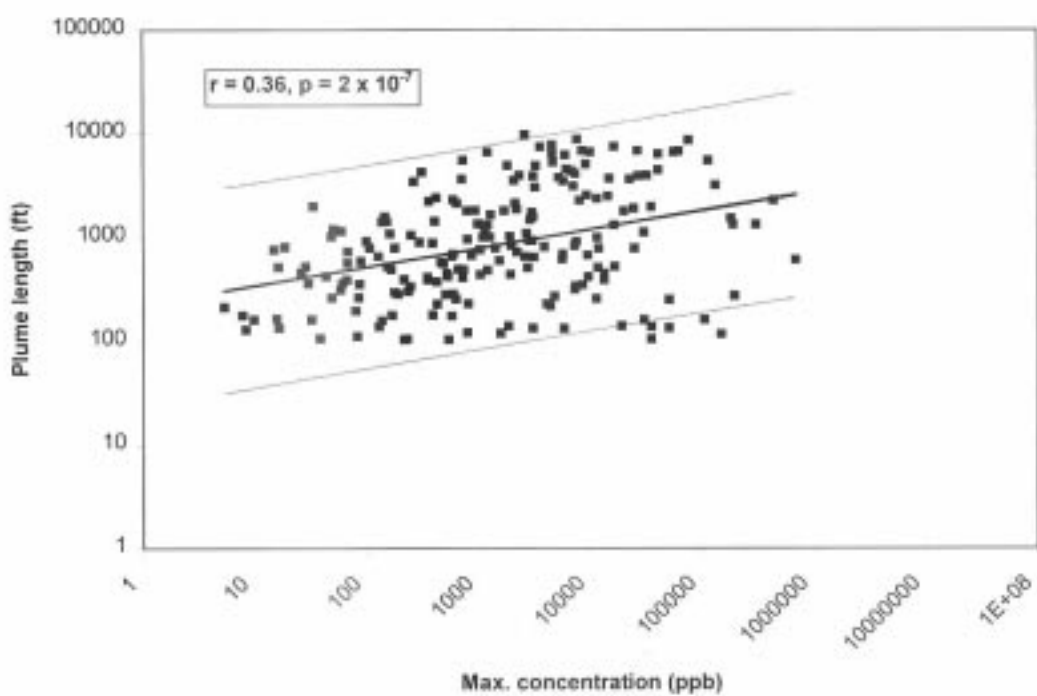
X

Figure G-2. Relationship between log plume length and log C_{max} for the synthetic 10-ppb plume population. Dashed lines denote the 95% prediction confidence band.
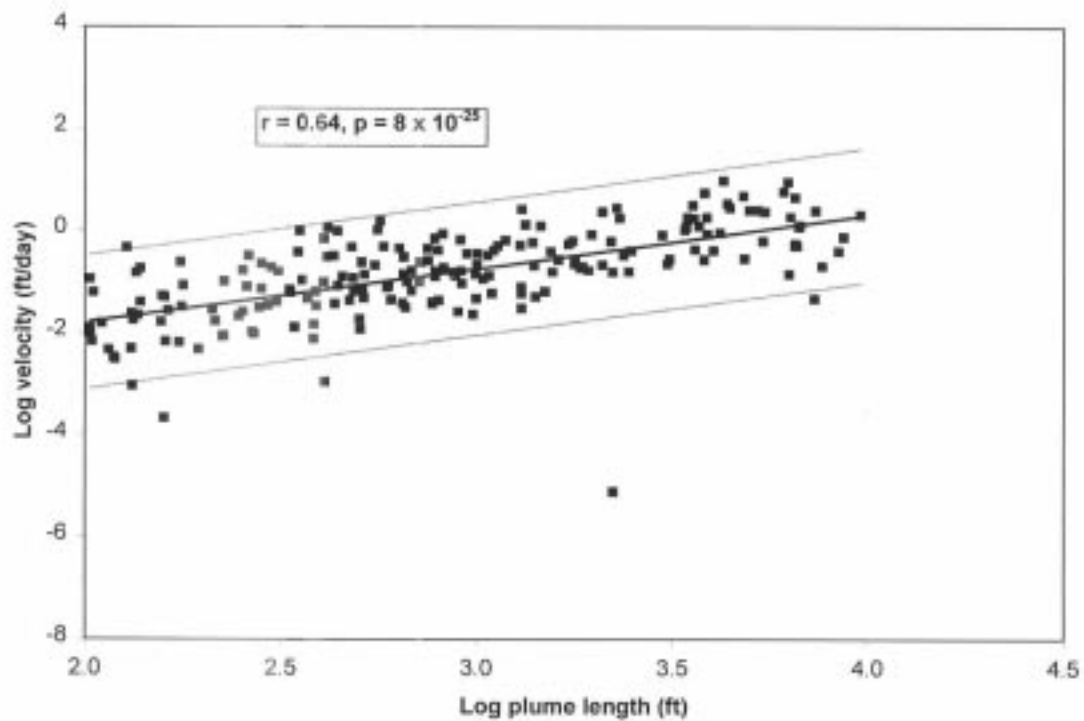
Figure G-3. Relationship between log plume length and log specified v from the synthetic plume. The independent variable, log v, is plotted on the y-axis to maintain consistency with Figure A-4. Dashed lines denote the 95% prediction confidence band.
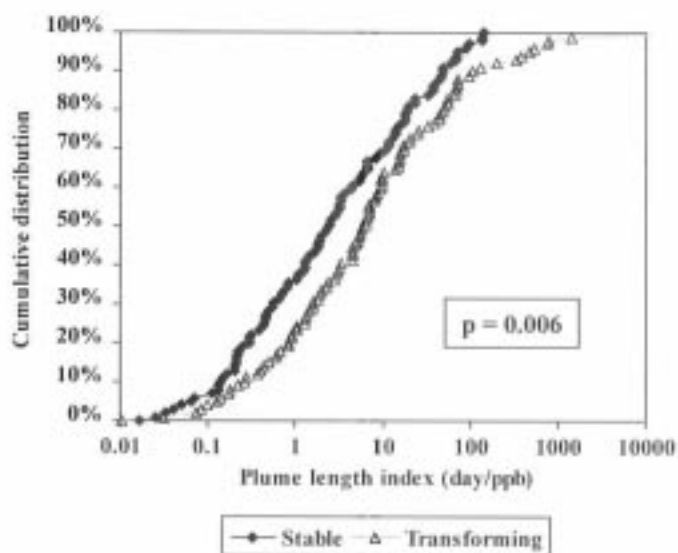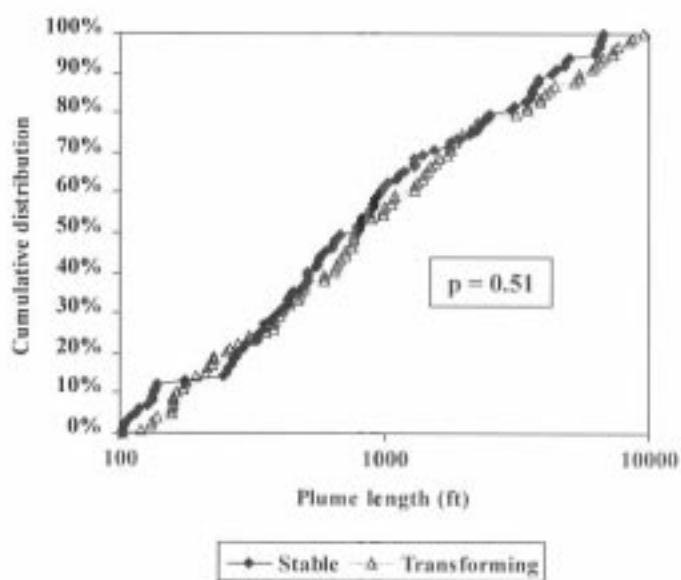
Figure G-4. Cumulative distributions of plume lengths for synthetic stable and transforming plumes (top), and distributions of plume length indices (bottom). *P*-values refer to the null hypothesis probability (i.e. the probability that the two data sets have equal geometric means).
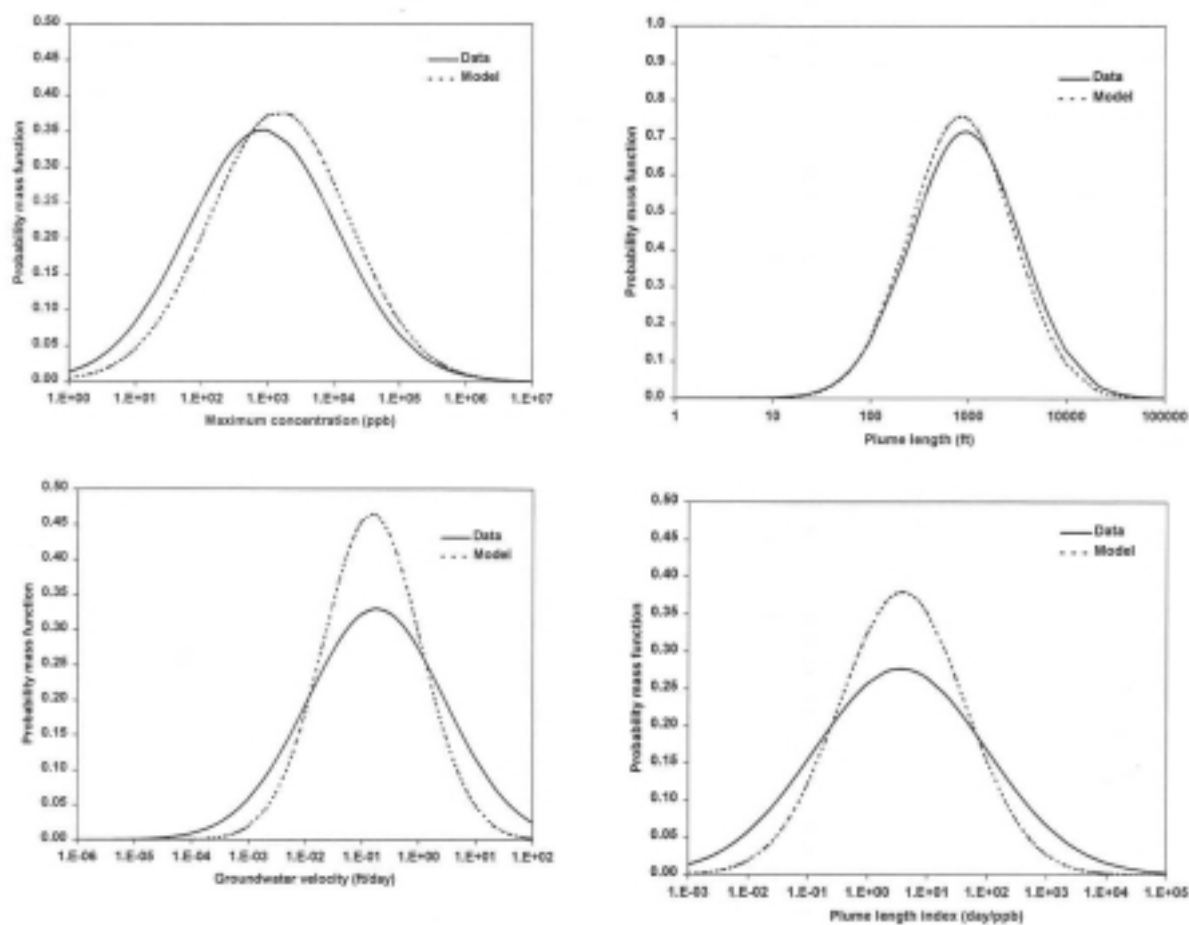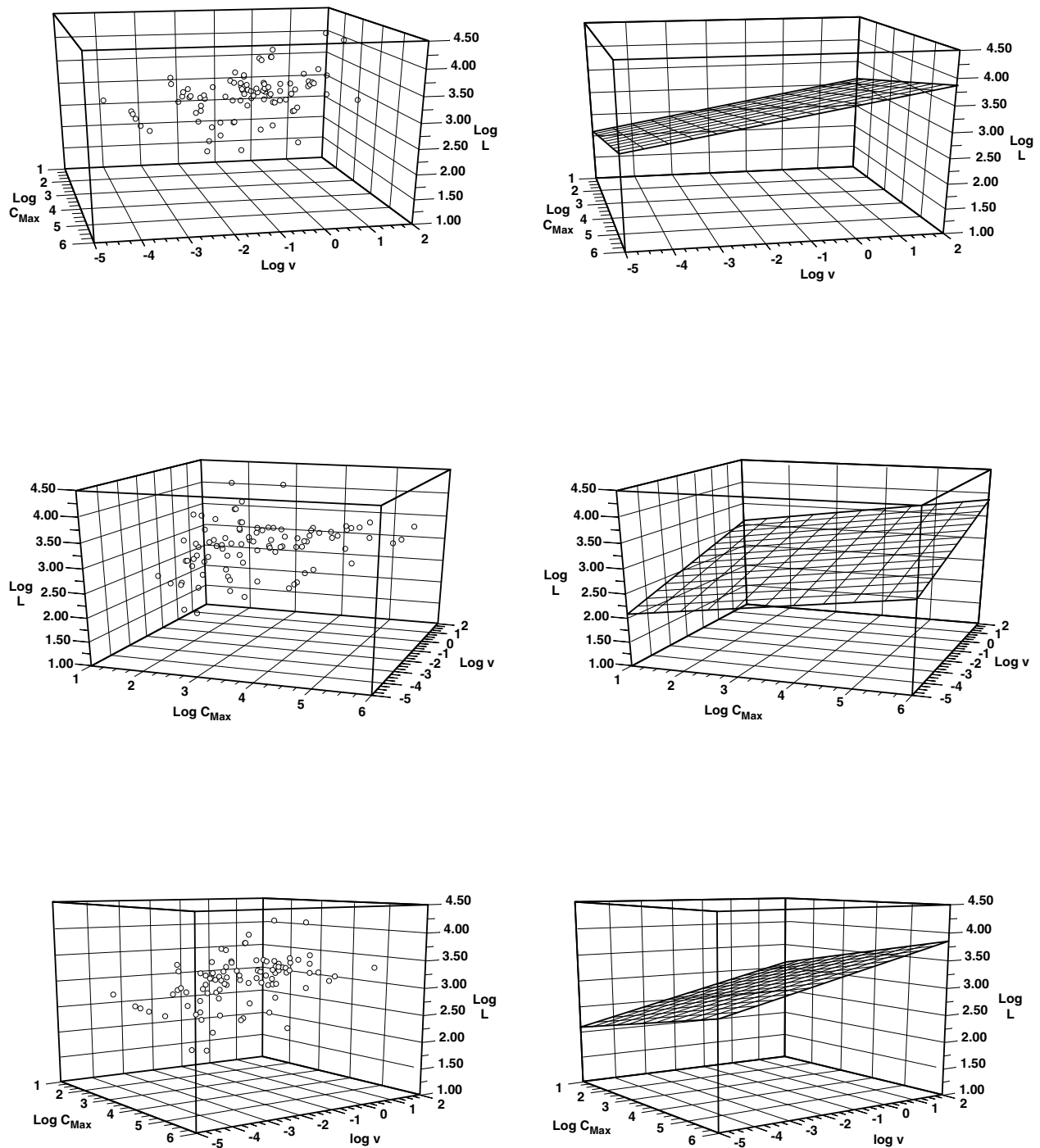
Figure G-5. Lognormal probability distributions for independent variables (maximum concentration and groundwater velocity) and dependent variables (plume length – 10 ppb – and plume length index) fit to the CVOC historical case data ("Data") and the synthetic plume population ("Model").

Figure G-6. Multivariate relationship between log hydraulic conductivity, log maximum historical concentration, and log plume length for measured data (viewed from multiple angles). Biotransformation was eliminated as a varible min this scatter plot by plotting only plumes from the No-RD group. Multivariate correlation coefficient: r= 0.48 (corresponding best-fit planar surface shown in right column).
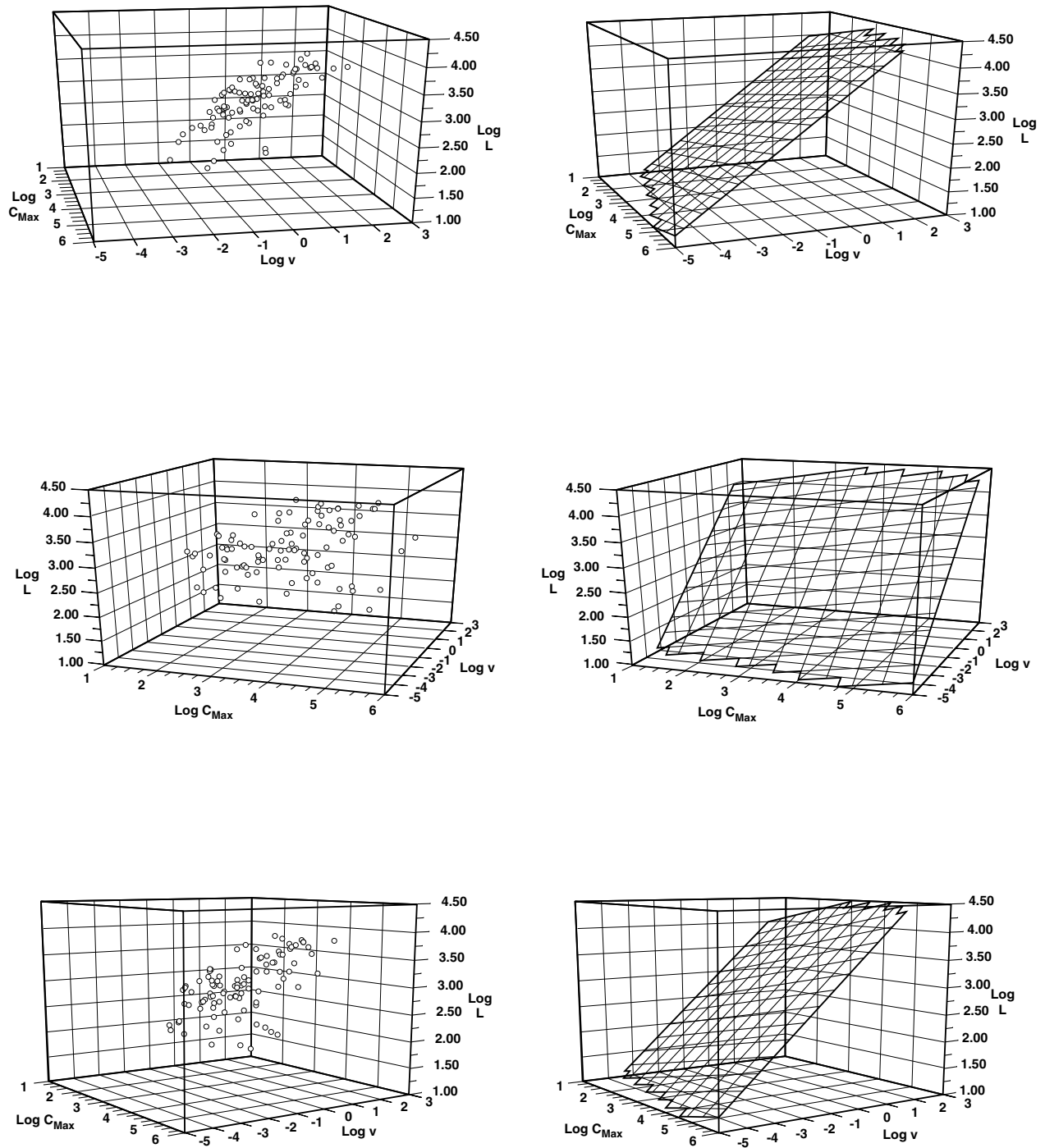
Figure G-7. Multivariate relationship between log hydraulic conductivity, log maximum historical concentration, and log plume length for synthetic plume population (viewed from multiple angles). Degradation was eliminated as a variable in this scatter plot by plotting only those plumes that were assigned a value of =0. Multivariate correlation coefficient: r= 0.83 (corresponding best-fit planar surface shown in right column).